ACS APPLIED MATERIALS & INTERFACES

Research Article

www.acsami.org

Foldable Transparent Substrates with Embedded Electrodes for Flexible Electronics

Jin-Hoon Kim and Jin-Woo Park*

Department of Materials Science and Engineering, Yonsei University, Seoul, 120-749, Korea

Supporting Information

ABSTRACT: We present highly flexible transparent electrodes composed of silver nanowire (AgNW) networks and silica aerogels embedded into UV-curable adhesive photopolymers (APPs). Because the aerogels have an extremely high surface-to-volume ratio, the enhanced van der Waals forces of the aerogel surfaces result in more AgNWs being uniformly coated onto a release substrate and embedded into the APP when mixed with an AgNW solution at a fixed concentration. The uniform distribution of the embedded composite electrodes of AgNWs and aerogels was verified by the Joule heating test. The APP with the composite electrodes has a lower sheet resistance (R_s) and a better mechanical stability compared with APP without aerogels. The APP with the embedded electrodes is a freestanding flexible substrate and can be used as an electrode coating on a polymer substrate, such as polydimethylsiloxane and polyethylene terephthalate. On the basis of the bending test results, the APPs with composite electrodes were sufficiently flexible to withstand a 1 mm bending radius (r_b) and could be foldable with a slight change in R_s. Organic light emitting diodes were successfully fabricated on the APP with the composite electrodes, indicating the strong potential of the proposed flexible TEs for application as highly flexible transparent conductive substrates.

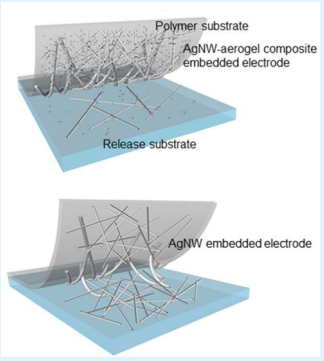

KEYWORDS: *foldable substrates, embedded electrode, Ag nanowires, aerogel, transparent electrode, organic light emitting diode*

1. INTRODUCTION

Electronic devices have evolved from their bulky, fixture-like origins to mobile appliances and flexible, textile, and stretchable electronics, which are referred to as soft electronics.[1] As the applications for soft electronics have expanded, the demand for high-quality flexible substrates has increased.[2] Commercial polymers, such as polyethylene terephthalate (PET) and polyimide (PI), have been considered the primary candidates for use as flexible substrates due to their low cost, high compliance, and ruggedness.[3] Many devices remain rigid because the functional coatings used for engineering polymer substrates, particularly transparent conductive electrodes (TCEs), generally consist of brittle oxides, which limit the flexibility of the substrates.[1]

Low-dimensional materials, such as graphene, carbon nanotubes (CNTs), metal nanowires, and their composites, have been investigated as flexible TCEs to replace transparent conductive oxide (TCO) electrodes.[4−6] These materials have greater flexibility on polymer substrates than do TCOs.[7,8] However, some of these materials have electrical and optical properties that are inferior to those of TCO.[4,9] Among the replacement candidates, silver nanowire (AgNW) networks (or meshes) are the most promising because they have better functional and mechanical properties compared with those of TCO and can be coated onto large-area flexible polymer substrates using various solution-coating technologies.[5]

Despite the advantages of AgNW networks as a replacement for TCO, there are a few technological hurdles to overcome in fabricating various devices with AgNW electrodes. First, AgNW meshes produce extremely rough surfaces (R_{rms}), which limit the uniform interfacial contact and chemical bond formation with the materials on top of the electrode.[10] Second, the nanowire networks have partially disconnected ends, resulting in electrical shorts in the device construction.[11] Finally, the AgNW areal density tends to be nonuniform, which results in variations in the R_s.

Recently, trends for AgNW-based electrodes include fabricating hybrid structures with other TCEs or polymer matrices to resolve the above-mentioned issues.[12−14] For example, AgNW-based hybrid electrodes coated with graphene, carbon nanotube, and poly(3,4-ethylenedioxythiophene)/poly-(styrenesulfonate) (PEDOT/PSS) have been reported.[10,14,15] This hybrid structure could improve the electrical properties and mechanical stability of the electrodes.[14,15] However, hybridization with other TCEs little improved the rough surfaces of AgNW networks and disconnected ends of AgNWs.[10]

The composite TCEs with polymer matrices, especially, the AgNWs embedded in deformable polymer substrates, have been suggested to effectively resolve the above-mentioned issues.[11,16] This approach provides a promising solution, particularly for the large R_{rms} and the electric shorting of coated AgNW networks.[12,17] For example, the successful fabrication of flexible organic solar cells (OSCs) and organic

Received: June 5, 2015
Accepted: August 10, 2015
Published: August 10, 2015

DOI: 10.1021/acsami.5b04982
ACS Appl. Mater. Interfaces 2015, 7, 18574−18580

light-emitting diodes (OLEDs) has been achieved on substrates with embedded AgNW networks.[10−12,17,18] However, the types of transparent polymer substrates in which AgNWs can be embedded are limited because the adhesion between the polymer and the AgNWs should be stronger than that between a release substrate and the AgNWs.[19] Hence, the low optical transmittance (T) of the polymer substrates is often compensated for by the reduced R_{rms} and the disconnected ends of the embedded AgNW networks. In addition, the issue of the nonuniform embedded AgNW areal density remains unresolved in AgNW coatings.[20]

For the fabrication of the AgNW-embedded substrates, Si or glass is most frequently used as the release substrate. When embedded, the adhesion of AgNWs to the release substrate and the polymers significantly affects the transfer efficiency of the AgNWs.[19] The ratio of the AgNWs transferred to the polymer substrate to those coated on the release substrate is often represented by the ratio of R_s of the embedded electrode to R_s of the electrode coating on the release substrate.[21] For the efficient detachment of the AgNWs from the release substrates, a sacrificial layer, such as poly(methyl methacrylate) (PMMA), has been coated between the release substrate and AgNW networks in a previous study.[12]

In this study, we used aerogels as a strong transfer medium for the AgNWs. Given the extremely high surface-to-volume ratio of the aerogels, a strong van der Waals interaction is expected between the aerogels and the AgNWs when the aerogels are thoroughly mixed with the AgNWs in a solution. After the liquid polymer was coated, aerogels form stronger van der Waals interaction between AgNWs and the polymer substrate than between AgNWs and the release substrate due to significantly increased contact areas. This will promote highly enhanced transfer of the AgNWs from the release substrate when embedded. The strong interaction will create denser AgNW networks coated onto the release substrate and will promote the detachment of the AgNWs from the release substrate during embedding. We selected a UV-curable adhesive photopolymer (APP) as the polymer substrate material for embedding in this study.

The APP can be used as a freestanding substrate and as a coating with embedded electrodes on other flexible polymer substrates, such as PDMS and PET.[2,11,16] In addition, the APP can easily make patterns for imprinting onto the surface. The composite electrodes of AgNWs and aerogels were embedded into the APP, and the electrical, optical, and mechanical properties of the APP with the embedded composite electrodes were compared with those of the APP with embedded AgNWs. To verify the potential applications of flexible substrates for optoelectronic devices, flexible OLEDs were fabricated on the APP with embedded composite electrodes.

2. EXPERIMENTAL SECTION

A 1 wt % AgNW solution (Nanopyxis, Seongnam, Korea) was diluted to the ranges of 0.15 to 0.3 wt %, and silica aerogels (JIOS Aerogel Corporation, Osan, Korea) were dispersed into the diluted solution. The concentration of aerogels (C_A) in the solution varied from 0.15 to 0.3 wt %. Solutions with various ratios of AgNW concentration (C_{Ag}) to C_A were spin-coated two or three times onto a Si wafer (which was used as the release substrate) at 1000 rpm for 60 s. Composite-type meshes of AgNWs and aerogels were formed on the substrate, and the solvent was evaporated by post-thermal annealing at 100 °C for 20 min. To evaluate the interaction forces among the AgNWs, the aerogels, and the Si release substrate, the scotch-tape test was performed for the AgNW meshes without aerogels and the composite meshes, and then the results were compared. The sheet resistance (R_s) values of the composite meshes and the AgNW networks were measured using a four-point probe.

We used the UV-curable APP (Norland Optical Adhesive 68 (NOA 68)) as the polymer substrate for embedding. The APP was spin-coated at 500 rpm for 60 s on the release substrate coated with electrodes and then cured using a UV lamp for 5 min. To fabricate composite coatings in PET substrate, the APP was spin-coated at 5000 rpm for 60 s on the release substrate coated with AgNWs and cured same to the above method. After being cured, the surfaces of the hybrid coatings and PET substrate were oxygen plasma treated at 140 W for 90 s. After that, hybrid coatings and PET were contacted and annealed at °C for 10 min to form a chemical bonding. To control the compliance of the polymer substrate, the cured polymer was heat-treated on a hot plate at 50 °C for 12 h. Next, the APP with embedded electrodes or hybrid coatings on PET was released from the Si substrate. Descriptions of the embedding process are schematically illustrated in Figure 1. The embedded electrode samples are described

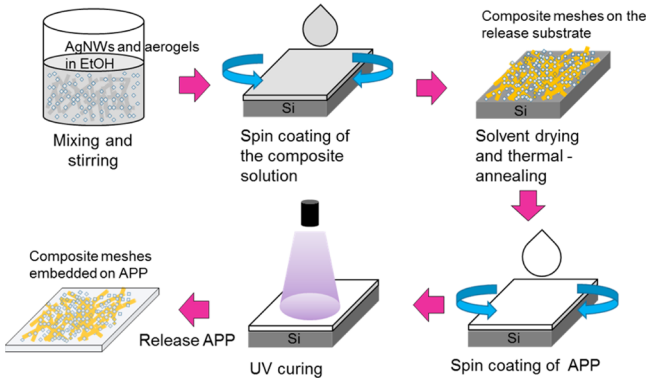

Figure 1. Schematic description of the embedding and coating processes.

in Table 1 in detail. The R_s and T values of the embedded electrodes were measured using the four-point probe and UV−visible spectroscopy, respectively.

Table 1. Sample Names and Detailed Descriptions of the Substrates with Embedded Electrodes

sample	AgNW concentration (wt %)	aerogel concentration (wt %)
Ag20	0.2	
C20	0.2	0.2
Ag25	0.25	
C25	0.25	0.25
Ag30	0.3	
C30	0.3	0.3

The microstructures of the AgNW networks and the composite meshes before and after embedding were analyzed using field emission−scanning electron microscopy (FE-SEM), high-resolution transmission electron microscopy (HR-TEM), and atomic force microscopy (AFM). Using optical microscopy (OM), the transfer rate was evaluated by observing the residual AgNWs on the release substrate after embedding. To confirm improvements in the distribution uniformity and the increased transfer rate of the AgNW meshes using aerogels, Joule heating experiments[9] were performed. In these Joule heating experiments, DC voltage was applied using a Keithley 2400 source meter through two silver paste (P-100, CANS) contacts at the edges of the electrode, and the temperatures of the polymer films with embedded electrodes were measured by an infrared thermal imager (IR camera). A current was induced for 120 s to attain a steady state. Finally, the electrical power was turned off, and the samples were cooled until reaching a temperature of 25 °C.

DOI: 10.1021/acsami.5b04982
ACS Appl. Mater. Interfaces 2015, 7, 18574−18580

The static and cyclic bending tests of the APP substrates with the embedded electrodes were performed to evaluate the mechanical reliability of the electrodes. In the static test, r_b is decreased to 1 mm, and the cyclic bending tests were performed at r_b of 5 mm and at a bending rate of 2 mm/s for up to 2000 cycles. AgNWs were coated onto PET, and the same static and cyclic tests as those performed on the APP were conducted. These test results were used to compare with the bending stability of the APP with embedded meshes. To test the foldability, light emitting diode (LED) bulbs were mounted on the flat and folded APP with the composite electrodes, and the electrical connectivity was examined.

OLEDs were fabricated on the bare AgNW networks and on the composite electrodes, Ag30 and C30 in Table 1, as the anode. The OLEDs were composed of 5 layers. The organic layers coated on the anode consisted of (1) PEDOT/PSS (Heraeus Clavios PVP AI 4083) as the hole transport layer (HTL), (2) SY-PPV (Super-Yellow by Merck) as the emission layer (EL), and (3) cesium carbonate (Cs_2CO_3, Sigma-Aldrich) as the electron transport layer (ETL). PEDOT/PSS solution with a weight ratio to 2-propanol was spin coated onto Ag30 and C30 at 1000 rpm and then heat treated at 100 °C for 5 min.

On top of the HTL, EL dissolved in toluene (5 mg/mL) was spin coated at 1500 rpm, followed by heat treatment at 100 °C for 5 min inside of a N_2-filled gloved box. Subsequently, 0.5 wt % Cs_2CO_3 in 2-ethoxyethanol was spin coated at 5000 rpm on top of the EL and then heat treated at 100 °C for 5 min. The samples were then removed from the glovebox and transferred to an evaporator chamber to deposit 150 nm Al films as the cathode. The current density (J) vs voltage (V) and luminescence (L) vs V characteristics of the OLEDs on Ag30 and C30 were measured using a Keithley 2400 SourceMeter and a Minolta CS-200 chromameter.

3. RESULTS AND DISCUSSION

Figure 2a shows the R_s value for AgNW meshes that were spin-coated onto the release substrate for varying values of C_{Ag} and C_A. The R_s values of the composite meshes for a fixed C_{Ag} are compared for varying values of C_A. According to Figure 2a, R_s decreased with an increase in C_{Ag}: 24 Ω/sq at 0.2 wt % and 11 Ω/sq at 0.3 wt %, for example. In addition, R_s decreases with

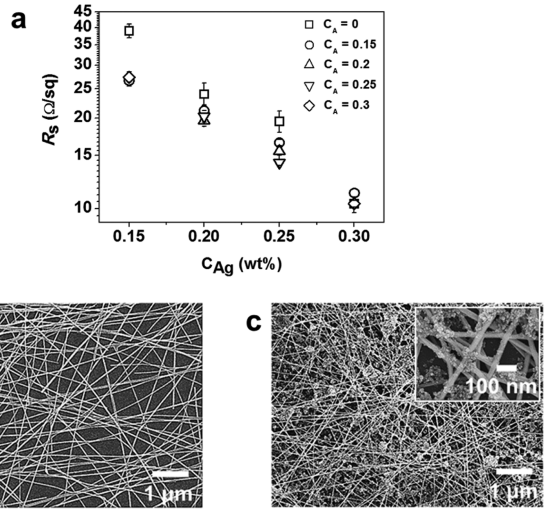

Figure 2. (a) R_s of AgNW networks coated on the Si substrate as a function of the AgNW concentration in the solution compared with the AgNWs coated with the aerogels; FE-SEM images of (b) AgNW mesh coating from the 0.25 wt % AgNW solution on Si and (c) composite meshes of the AgNWs and aerogels (0.25 wt % AgNWs and 0.25 wt % aerogel). The inset image in (c) shows a magnification of the meshes, which confirms that the aerogels preferentially adhered to the AgNWs over the substrates.

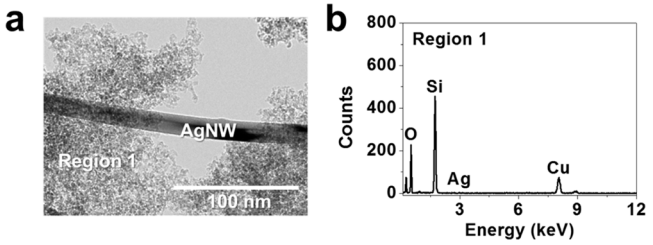

Figure 3. (a) HR-TEM image of the AgNWs and the aerogels attached to the AgNWs on the scotch-tape, (b) energy dispersive spectroscopy (EDS) analysis results of Region 1 in (a), which are aerogels adjacent to the AgNWs in the composite meshes.

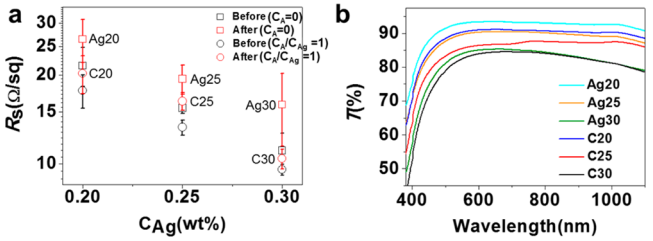

Figure 4. (a) Comparison of the R_s values of the composite meshes and the AgNW networks coated on Si release substrates ("before" embedding) with the R_s values of the polymer substrates with embedded electrodes ("after" embedding) and (b) comparison of the T values of the APP with the embedded AgNW network with those of the APP with the composite meshes.

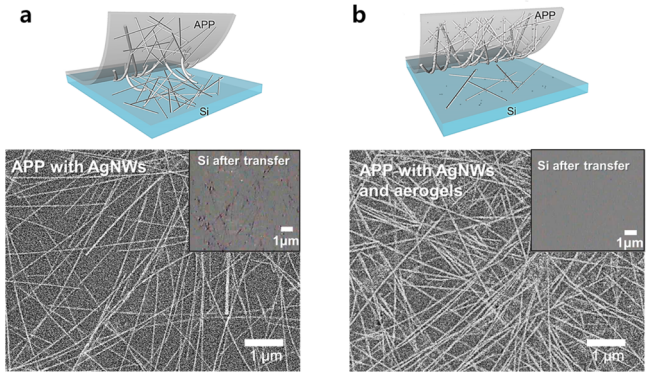

Figure 5. Schematic descriptions of the transferring process, FE-SEM images, and OM images (the inset OM images embedded in the FE-SEM images) comparing the transfer rate of AgNWs in (a) Ag30 with in (b) C30 described in Table 1.

increasing C_A for all C_{Ag}. For example, the R_s of the composite mesh coated with a solution of 0.15 wt % AgNWs decreased to that of the bare AgNW meshes from the 0.2 wt % AgNW solution. However, the effect of the aerogels on R_s is greater for a smaller C_{Ag}. As shown in Figure 2a, the difference in R_s for the composite and bare AgNWs decreases with increasing C_{Ag} and becomes nearly negligible at 0.3 wt %. According to our experiment, the aerogels had a minimal effect on reducing R_s for C_{Ag} values above 0.3 wt %.

On the basis of Figure 2a, the optimal ratio of C_A to C_{Ag} for maximizing the effect of the aerogels on reducing R_s was 1. Above the threshold ratio of 1, the R_s value of the composite meshes either increases slightly or becomes saturated. The FE-SEM images in Figure 2, parts b and c, which show a comparison of the AgNW meshes with and without aerogels (C_A/C_{Ag} = 1), reveal that a denser AgNW mesh was coated on

DOI: 10.1021/acsami.5b04982
ACS Appl. Mater. Interfaces 2015, 7, 18574−18580

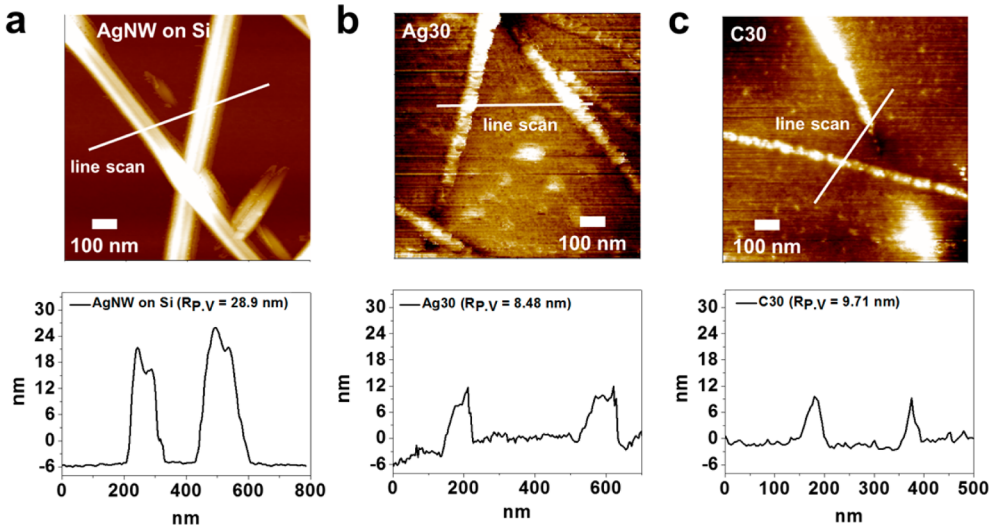

Figure 6. AFM images of the surface of the electrodes, the line-scan data across the surfaces, and the average R_{rms} in (a) AgNW networks on Si, (b) Ag30 in Table 1, and (c) C30 in Table 1.

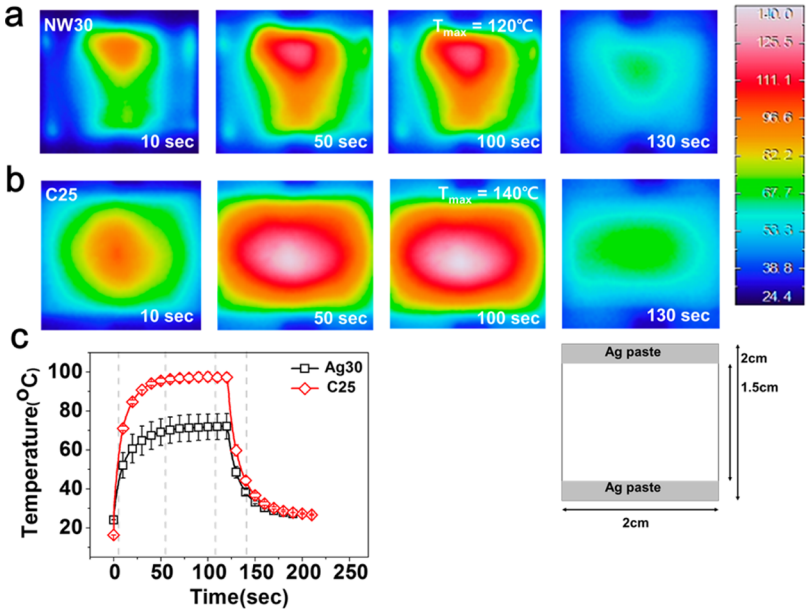

Figure 7. Transient IR images showing the temperature distributions over the sample areas during the Joule heating tests for comparing the uniform embedding and distributions of the AgNWs in the embedded substrates (a) without aerogels (Ag30) and (b) with aerogels (C25); and (c) the average temperature variation as a function of time in Ag30 and C25.

the substrate with the aerogels. This result clearly demonstrates the effect of aerogels on flocculating AgNWs with strong van der Waals forces, which improved the coating density and uniformity of AgNWs on the release substrate. As presented in Figure 2b, the aerogels were uniformly distributed over and between the AgNWs. The inset image with a higher magnification clearly shows that the aerogels adhered primarily to the AgNW meshes, with only a light coating on the substrate.

To confirm the strong attraction between the AgNWs and the aerogels, AgNW meshes with and without aerogels were mechanically detached from the release substrates via the scotch-tape test, as schematically described in Figure S1, parts a and b. The test results are summarized in Figure S1, parts a and b, showing the OM images of the electrode coatings before and after performing the scotch-tape test. For the AgNW coatings without the aerogels (Figure S1a), a few AgNW meshes were detached by scotch-tape as determined by comparing Region I and Region II in Figure S1a. In contrast, the densely coated composite meshes in Region III (Figure S1b) were nearly completely removed from the release substrate by the tape test, as shown in Region IV in Figure S1b. This result indicates that aerogels help transfer AgNWs from the release substrate by strong van der Waals interaction with AgNWs and polymer matrices. The composite meshes on the scotch-tape were forcefully detached using a razor blade and then transferred to a Cu grid for HR-TEM analysis. As expected, the AgNWs were lifted with the aerogels, as shown in the HR-TEM image in Figure 3a. The EDS point analysis shown in Figure 3b verifies that the particles near the AgNWs are aerogels. The Cu peak in Figure 3b results from the Cu grid.

DOI: 10.1021/acsami.5b04982
ACS Appl. Mater. Interfaces 2015, 7, 18574−18580

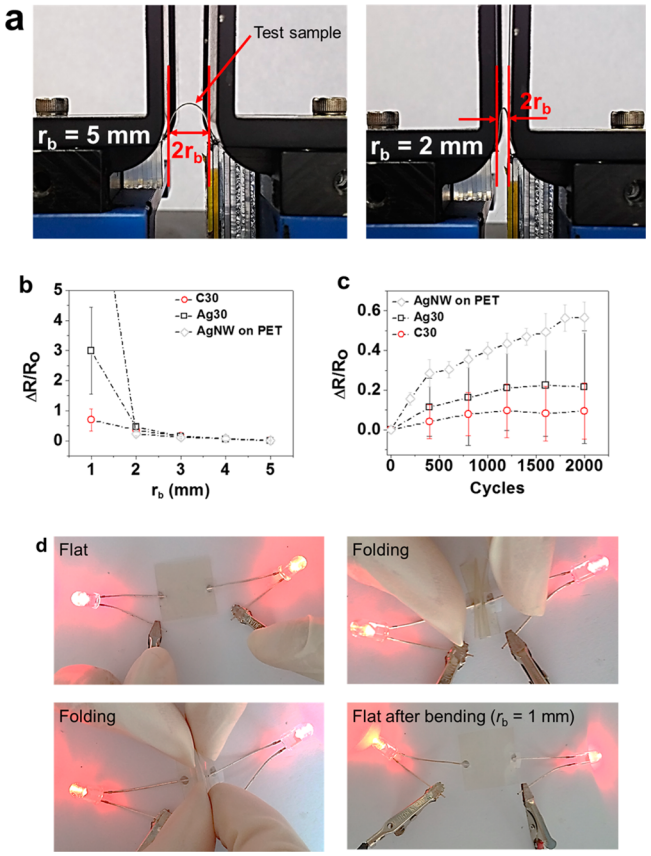

Figure 8. (a) The bending tester, (b) static, and (c) cyclic bending test results for Ag30 and C30 compared to AgNW coated on PET; and (d) photographs of red LED diodes mounted on C30 under various conditions, including being flat during folding and bending (r_b = 1 mm).

Table 2. Luminance Changes of the LED Light after Folding

	red LED (cd/m^2)	yellow LED (cd/m^2)
initial state	205 889	141 640
folding state	184 748	141 736

Figure 4a presents the variation in R_s for the AgNW networks and the composite meshes after embedding. In the composite meshes, the ratio of C_A to C_{Ag} was 1. After embedding, the R_s values of Ag20, Ag25, and Ag30, presented in Table 1, increased by more than 30% on average compared with the AgNWs on the Si substrate (Figure 4a). In addition, the maximum variation in the R_s value of the specimens for each sample is 19%, as demonstrated by the standard deviations in Figure 4a. Conversely, the R_s values of C20 and C25 increased by only 14% and 22% compared with Ag20 and Ag25, respectively. The variation in the R_s value of C30 was nearly negligible, as shown in Figure 4a, indicating that most of the coated AgNWs on Si were transferred into the APP.

Figure 4b shows the T values for the samples in Table 1. The T values of the AgNW networks generally decrease with the increasing density of the networks. As shown in Figure 4b, the average T values for the samples of lower R_s (Figure 4a) are higher, except for C30. Aerogels over a certain concentration appear to affect T. The electrical and optical properties of the embedded composite meshes are superior to those of another embedded electrode based on AgNWs and APP previously fabricated by others.[11]

The schematic descriptions of the transferring process, FE-SEM images, and OM images displayed in Figure 5, parts a and b, provide a comparison of the residual AgNWs on the release substrates after fabricating Ag30 and C30 (Table 1), respectively. Figure 5, parts a and b, confirms the significantly improved transfer efficiency of AgNWs with the aerogels. As shown in the inset OM image in Figure 5a, a substantial amount of AgNWs remained on the release substrate for Ag30, whereas few residual AgNWs were detected on the surfaces of the Si for C30, as shown in Figure 5b. According to Figure 5, parts a and b, the AgNWs in C30 appear to be denser and more uniformly distributed than do those in Ag30.

The AFM measurement results (surface images and line-scanned data) of the embedded AgNWs are compared with those of the AgNW networks coated on Si in Figure 6, parts a–c. R_{rms} of the embedded electrodes are less than one-third of that of the coated AgNWs on Si, according to the results in Figure 6a–c. There is a negligible difference in R_{rms} of the embedded electrodes with and without aerogels. The surface morphology of the electrodes significantly affects the device performances because the interfacial contact with the subsequently coated organic layers on top of the electrode tends to degrade with increasing R_{rms}.[10] Hence, the reduced R_{rms} of the AgNW electrode surface by embedding is expected to improve the potential application of the APP with the electrodes for flexible substrates.

In addition to the transfer efficiency, the distribution uniformities of the embedded AgNWs without and with aerogels, Ag30 and C25 (Table 1), respectively, were compared by Joule heating tests, and the test results are shown in Figure 7. On the basis of Figure 4a, Ag30 and C25 exhibit nearly the same average R_s values and are expected to have similar areal densities of AgNWs. In Figure 7, parts a and b, the temperature distributions of Ag30 and C25 are compared for heating and cooling. If the AgNWs were embedded uniformly throughout the substrate surfaces, then the temperature distribution on the sample surfaces would theoretically decrease radially from the center to the edges. However, this trend was not observed in Ag30. Note that heating occurred in a limited area of Ag30 because of the nonuniform embedding of the AgNWs, while heating occurred uniformly throughout the areas of C25. Due to the uniform heating, the maximum temperature is higher in C25 than in Ag30, as shown in Figure 7c. This result clearly verifies the highly enhanced uniformity in the distribution of the embedded AgNWs for the composite electrodes with aerogels compared with the AgNWs without aerogels.

The bending tester is shown in Figure 8a, and the static and cyclic bending test results for the embedded composite meshes are compared with those for the embedded AgNW networks and coated AgNWs on PET in Figure 8, parts b and c, respectively. In the static bending tests (Figure 8b), C30 showed the highest bending stability over the other two samples. R_s of the AgNWs on PET drastically increased as r_b is decreased less than 2 mm. At 1 mm r_b, the change in R_s of Ag30 is more than three times larger than that of C30. In the cyclic bending tests, the R_s changes for the AgNWs on PET were significantly higher than those of Ag30 and C30 for all cycles (Figure 8c). While the increases in R_s of Ag30 and C30 are saturated over 1000 cycles, the R_s of AgNWs on PET continues to increase over the cycles.

For 2000 cycles at 5 mm r_b, C30 showed greater mechanical stability than Ag30, as shown in Figure 8c. The R_s value for C30 increased by 9.5% (1 Ω/sq) over 2000 cycles, whereas the

DOI: 10.1021/acsami.5b04982
ACS Appl. Mater. Interfaces 2015, 7, 18574–18580

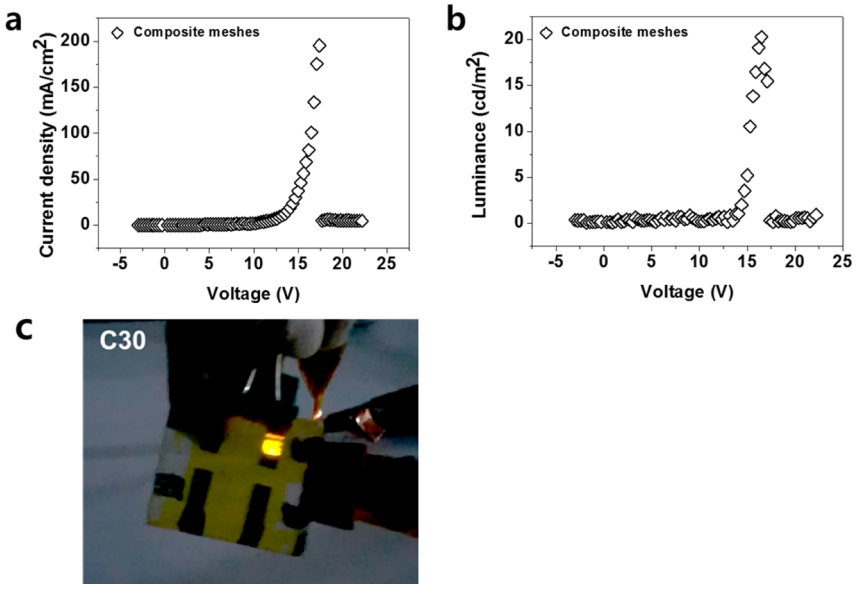

Figure 9. (a) The $J-V$ curve and (b) the $L-V$ curve of the OLEDs fabricated on C30; and (c) photograph of the emission from the OLED based on C30 operated at 14 V.

increase in R_s for Ag30 was 22% (5 Ω/sq), as presented in Figure 8c. These results clearly indicate the role of aerogels in preventing the AgNWs from being separated at the junctions under the out of plane stresses induced by bending that push forward or backward through the thickness of the substrates. Also, aerogels could improve binding between AgNWs and APP matrices, which could prevent deformation of AgNWs like detachment or protrusion. As shown in Figure 8d, electrical connection of C30 is well maintained on bending at r_b of 1 mm and when folded to have the characteristics of the flat state. LED lights remained turned on under the various conditions in Figure 8d, with little change in brightness (Table 2).

To analyze the change in the brightness of the LEDs when the substrate was folded, the luminescence of the LEDs was measured using chromameter in the dark box. As shown in Table 2, the changes in luminescence of both yellow and red LEDs were almost negligible. In Figure S2, the images of initial and folded states of the substrates used in measuring the luminance of the LEDs are shown. Movie S1 shows the folding operation of the substrates.

One of the simple ways to decrease the bending stress induced in the film is to decrease the thickness of the films.[22] In this study, the thickness of the composite electrodes was 210 μm. If the thickness of the composite electrodes become thinner, then better bending stability is expected. However, with less than a certain thickness, which may be a threshold thickness, the composite film can lose its mechanical stability as a free-standing film.

According to the previously reported work by Miller et al.,[16] AgNW-based hybrid coatings on the substrates such as PET and PDMS could be used as stretchable electrodes.[16] Gaynor et al. reported hybrid electrode based on AgNWs and PEDOT/PSS.[10] In this work, the R_{rms} value could be reduced by PEDOT/PSS; however, the electrical and optical properties were degraded. Kim et al. reported freestanding hybrid electrodes with AgNWs and optical adhesive.[11] The optical properties of the hybrid TCEs by Kim et al. was comparable to C30 in this work. However, the electrical and mechanical properties of C30 are highly enhanced with the aerogels compared to the hybrid TCEs by Kim et al.[11]

OLEDs were fabricated on C30, and $J-L-V$ characteristics of the OLEDs on C30 are summarized in Figure 9, parts a and b, respectively. As shown in Figure 9a, the $J-V$ relationship is as good as that measured in the flexible OLEDs on the composite electrode of AgNWs and Ag films in a previous work by the current authors.[17] Considering the fact that the previously developed composite electrodes were almost continuous films, the result in Figure 9a should be noted. However, the turn-on V (V_{on}) at 1 cd/m^2 was measured to be as high as 13.8 V. According to Figure 9b, the maximum L is smaller by more than an order of magnitude than those on the ITO glass and the composite electrodes with AgNWs.[18] These differences may be the result of multiple reasons, with the primary causes attributed to the optical loss due to absorption by AgNWs within the visible ranges, low contact area between AgNWs and active polymer layers because of embedded AgNWs, and the low hole mobility of AgNWs;[12,23] these issues should be addressed in our ongoing works. Figure 9c is the image captured from video clips that recorded the performances of the f-OLEDs.

4. CONCLUSIONS

A significantly high transfer efficiency and uniform embedding of AgNW percolation mesh electrodes can be achieved by simply mixing aerogels with an AgNW solution because of the strong interaction between aerogels with an extremely large surface-to-volume ratio and AgNWs. As a result, the R_s value of the embedded electrodes was found to be significantly lower than that of bare AgNWs for a fixed AgNW concentration. In addition, the polymer substrates with the composite electrodes with aerogels were proven to be more highly stable under repetitive bending than the substrates with bare AgNWs and to be even foldable with little change in R_s. The film manufacturing processes that we have developed can also be used for large-area coatings. In addition, the polymer films developed in this study can be used as both freestanding substrates and coatings on other polymer substrates into which

DOI: 10.1021/acsami.5b04982
ACS Appl. Mater. Interfaces 2015, 7, 18574−18580

embedding electrodes is not possible. Successful fabrication of OLEDs on the substrates proves the potential application as the transparent conductive substrates for various soft electronic devices.

■ ASSOCIATED CONTENT

Supporting Information

Figures and movies of additional experimental data. The Supporting Information is available free of charge via the Internet at The Supporting Information is available free of charge on the ACS Publications website at DOI: 10.1021/acsami.5b04982.

(Figure S1) The OM images of the (a) AgNWs and (b) the composite meshes on the release substrates before and after the adhesion tests using scotch-tape; (Figure S2) photographs of red and yellow LED diodes mounted on C30 under flat and folded state(PDF)

(Movie S1) Folding and releasing of a C30 electrodes connected to a LED diodes (AVI)

■ AUTHOR INFORMATION

Corresponding Author

*Phone: +82 2 2123 5834; fax: +82 2 2123 5834; e-mail: jwpark09@yonsei.ac.kr (J.-W.P.).

Notes

The authors declare no competing financial interest.

■ ACKNOWLEDGMENTS

This work was supported by the Business for Cooperative R&D between Industry, Academy, and Research Institute (grant no. C0188503), which was funded by the Korea Small and Medium Business Administration in 2014.

■ REFERENCES

(1) Kaltenbrunner, M.; Sekitani, T.; Reeder, J.; Yokota, T.; Kuribara, K.; Tokuhara, T.; Drack, M.; Schwodiauer, R.; Graz, I.; Bauer-Gogonea, S.; Bauer, S.; Someya, T. An Ultra-Lightweight Design for Imperceptible Plastic Electronics. *Nature* **2013**, *499* (7459), 458−463.

(2) Li, Y.; Cui, P.; Wang, L.; Lee, H.; Lee, K.; Lee, H. Highly Bendable, Conductive, and Transparent Film by an Enhanced Adhesion of Silver Nanowires. *ACS Appl. Mater. Interfaces* **2013**, *5* (18), 9155−9160.

(3) MacDonald, B. A.; Rollins, K.; MacKerron, D.; Rakos, K.; Eveson, R.; Hashimoto, K.; Rustin, B. Engineered Films for Display Technologies. In *Flexible Flat Panel Displays*; John Wiley & Sons, Ltd.: New York, 2005; pp 11−33.

(4) Hecht, D. S.; Hu, L.; Irvin, G. Emerging Transparent Electrodes Based on Thin Films of Carbon Nanotubes, Graphene, and Metallic Nanostructures. *Adv. Mater.* **2011**, *23* (13), 1482−1513.

(5) Daniel, L.; Gaël, G.; Céline, M.; Caroline, C.; Daniel, B.; Jean-Pierre, S. Flexible Transparent Conductive Materials Based on Silver Nanowire Networks: A review. *Nanotechnology* **2013**, *24* (45), 452001−452020.

(6) Cheong, H.-G.; Triambulo, R. E.; Lee, G.-H.; Yi, I.-S.; Park, J.-W. Silver Nanowire Network Transparent Electrodes with Highly Enhanced Flexibility by Welding for Application in Flexible Organic Light-Emitting Diodes. *ACS Appl. Mater. Interfaces* **2014**, *6* (10), 7846−7855.

(7) Han, T.-H.; Lee, Y.; Choi, M.-R.; Woo, S.-H.; Bae, S.-H.; Hong, B. H.; Ahn, J.-H.; Lee, T.-W. Extremely Efficient Flexible Organic Light-Emitting Diodes with Modified Graphene Anode. *Nat. Photonics* **2012**, *6* (2), 105−110.

(8) Chen, R.; Das, S. R.; Jeong, C.; Khan, M. R.; Janes, D. B.; Alam, M. A. Co-Percolating Graphene-Wrapped Silver Nanowire Network for High Performance, Highly Stable, Transparent Conducting Electrodes. *Adv. Funct. Mater.* **2013**, *23* (41), 5150−5158.

(9) Yoon, Y. H.; Song, J. W.; Kim, D.; Kim, J.; Park, J. K.; Oh, S. K.; Han, C. S. Transparent Film Heater Using Single-Walled Carbon Nanotubes. *Adv. Mater.* **2007**, *19* (23), 4284−4287.

(10) Gaynor, W.; Burkhard, G. F.; McGehee, M. D.; Peumans, P. Smooth Nanowire/Polymer Composite Transparent Electrodes. *Adv. Mater.* **2011**, *23* (26), 2905−2910.

(11) Nam, S.; Song, M.; Kim, D. H.; Cho, B.; Lee, H. M.; Kwon, J. D.; Park, S. G.; Nam, K. S.; Jeong, Y.; Kwon, S. H.; Park, Y. C.; Jin, S. H.; Kang, J. W.; Jo, S.; Kim, C. S. Ultrasmooth, Extremely Deformable and Shape Recoverable Ag Nanowire Embedded Transparent Electrode. *Sci. Rep.* **2014**, *4*, 1−7.

(12) Ok, K.-H.; Kim, J.; Park, S.-R.; Kim, Y.; Lee, C.-J.; Hong, S.-J.; Kwak, M.-G.; Kim, N.; Han, C. J.; Kim, J.-W. Ultra-Thin and Smooth Transparent Electrode for Flexible and Leakage-Free Organic Light-Emitting Diodes. *Sci. Rep.* **2015**, *5*, 1−8.

(13) Lee, S.; Shin, S.; Lee, S.; Seo, J.; Lee, J.; Son, S.; Cho, H. J.; Algadi, H.; Al-Sayari, S.; Kim, D. E.; Lee, T. Ag Nanowire Reinforced Highly Stretchable Conductive Fibers for Wearable Electronics. *Adv. Funct. Mater.* **2015**, *25* (21), 3114−3121.

(14) Lee, M.-S.; Kim, J.; Park, J.; Park, J.-U. Studies on the Mechanical Stretchability of Transparent Conductive Film Based on Graphene-Metal Nanowire Structures. *Nanoscale Res. Lett.* **2015**, *10* (1), 1−9.

(15) Lee, P.; Ham, J.; Lee, J.; Hong, S.; Han, S.; Suh, Y. D.; Lee, S. E.; Yeo, J.; Lee, S. S.; Lee, D.; Ko, S. H. Highly Stretchable or Transparent Conductor Fabrication by a Hierarchical Multiscale Hybrid Nanocomposite. *Adv. Funct. Mater.* **2014**, *24*, 5671−5678.

(16) Miller, M. S.; O'Kane, J. C.; Niec, A.; Carmichael, R. S.; Carmichael, T. B. Silver Nanowire/Optical Adhesive Coatings as Transparent Electrodes for Flexible Electronics. *ACS Appl. Mater. Interfaces* **2013**, *5* (20), 10165−10172.

(17) Triambulo, R. E.; Cheong, H.-G.; Park, J.-W. All-Solution-Processed Foldable Transparent Electrodes of Ag Nanowire Mesh and Metal Matrix Films for Flexible Electronics. *Org. Electron.* **2014**, *15* (11), 2685−2695.

(18) Yu, Z.; Zhang, Q.; Li, L.; Chen, Q.; Niu, X.; Liu, J.; Pei, Q. Highly Flexible Silver Nanowire Electrodes for Shape-Memory Polymer Light-Emitting Diodes. *Adv. Mater.* **2011**, *23* (5), 664−668.

(19) Wang, J.; Yan, C.; Kang, W.; Lee, P. S. High-Efficiency Transfer of Percolating Nanowire Films for Stretchable and Transparent Photodetectors. *Nanoscale* **2014**, *6* (18), 10734−10739.

(20) Liang, J.; Li, L.; Tong, K.; Ren, Z.; Hu, W.; Niu, X.; Chen, Y.; Pei, Q. Silver Nanowire Percolation Network Soldered with Graphene Oxide at Room Temperature and Its Application for Fully Stretchable Polymer Light-Emitting Diodes. *ACS Nano* **2014**, *8* (2), 1590−1600.

(21) Li, L.; Liang, J.; Chou, S.-Y.; Zhu, X.; Niu, X.; ZhibinYu; Pei, Q. A Solution Processed Flexible Nanocomposite Electrode with Efficient Light Extraction for Organic Light Emitting Diodes. *Sci. Rep.* **2014**, *4*, 1−8.

(22) Röll, K. Analysis of Stress and Strain Distribution in Thin Films and Substrates. *J. Appl. Phys.* **1976**, *47* (7), 3224−3229.

(23) Triambulo, R. E.; Park, J.-W. Electronic Properties of Transparent Nano-Composite Electrodes for Application in Flexible Electronics. *Curr. Appl. Phys.* **2015**, *15* (Supplement 1), S12−S16.

DOI: 10.1021/acsami.5b04982
ACS Appl. Mater. Interfaces 2015, 7, 18574−18580